

# Indirect three-dimensional printing: A method for fabricating polyurethane-urea based cardiac scaffolds

R. Hernández-Córdova,<sup>1</sup> D.A. Mathew,<sup>2</sup> R. Balint,<sup>3</sup> H.J. Carrillo-Escalante,<sup>1</sup> J.M. Cervantes-Uc,<sup>1</sup> L.A. Hidalgo-Bastida,<sup>2</sup> F. Hernández-Sánchez<sup>1</sup>

<sup>1</sup>Centro de Investigación Científica de Yucatán, A.C., Mérida, Yucatán, México

<sup>2</sup>School of Healthcare Sciences, Manchester Metropolitan University, Manchester, United Kingdom

<sup>3</sup>School of Materials, University of Manchester, Manchester, United Kingdom

Received 30 September 2015; revised 8 March 2016; accepted 15 March 2016

Published online 4 April 2016 in Wiley Online Library (wileyonlinelibrary.com). DOI: 10.1002/jbm.a.35721

**Abstract:** Biomaterial scaffolds are a key part of cardiac tissue engineering therapies. The group has recently synthesized a novel polycaprolactone based polyurethane-urea copolymer that showed improved mechanical properties compared with its previously published counterparts. The aim of this study was to explore whether indirect three-dimensional (3D) printing could provide a means to fabricate this novel, biodegradable polymer into a scaffold suitable for cardiac tissue engineering. Indirect 3D printing was carried out through printing water dissolvable poly(vinyl alcohol) porogens in three different sizes based on a wood-stack model, into which a polyurethane-urea solution was pressure injected. The porogens were removed, leading to soft polyurethane-urea scaffolds with regular tubular pores. The scaffolds were characterized for their compressive and tensile mechanical behavior; and their degradation was monitored for 12 months

under simulated physiological conditions. Their compatibility with cardiac myocytes and performance in novel cardiac engineering-related techniques, such as aggregate seeding and bi-directional perfusion, was also assessed. The scaffolds were found to have mechanical properties similar to cardiac tissue, and good biocompatibility with cardiac myocytes. Furthermore, the incorporated cells preserved their phenotype with no signs of de-differentiation. The constructs worked well in perfusion experiments, showing enhanced seeding efficiency. © 2016 The Authors Journal of Biomedical Materials Research Part A Published by Wiley Periodicals, Inc. J Biomed Mater Res Part A: 104A: 1912–1921, 2016.

**Key Words:** indirect 3D printing, rapid prototyping, scaffold fabrication, polyurethane-urea, cardiac tissue engineering

**How to cite this article:** Hernández-Córdova R, Mathew DA, Balint R, Carrillo-Escalante HJ, Cervantes-Uc JM, Hidalgo-Bastida LA, Hernández-Sánchez F. 2016. Indirect three-dimensional printing: A method for fabricating polyurethane-urea based cardiac scaffolds. J Biomed Mater Res Part A 2016;104A:1912–1921.

## INTRODUCTION

According to the World Health Organization cardiovascular diseases have been the leading cause of death globally, claiming 17 million lives per year, more deaths than all cancers combined.<sup>1</sup> Furthermore, the impact of cardiovascular diseases is expected to grow further as the population ages.<sup>2</sup>

With the currently available therapeutic options, very few patients regain full cardiac function with no long-term side effects following cardiovascular damage.<sup>3</sup> Novel tissue engineering based treatments promise to overcome these limitations, by replacing injured cardiac tissue with artificially created fully functioning muscle and/or inducing endogenous cardiac regeneration.<sup>3</sup>

A key part of tissue engineered products are the biomaterial scaffolds. These are required to provide mechanical

support, and physical and biological cues for the viability, differentiation and correct architecture of the artificial tissue constructs.<sup>3</sup> However, none of the currently used cardiac scaffolds satisfy all of these requirements at the same time: Some do not possess the required architecture, lacking uniform pore size and porosity, or mechanical properties in correlation with that of heart tissue, while others are not biodegradable or do not show sufficient biocompatibility.<sup>3–5</sup>

Our group has recently synthesized a novel polycaprolactone (PCL) based polyurethane-urea (PUU) copolymer with putrescine as the chain extender.<sup>6</sup> Chain extenders are low molecular mass compounds (hydroxyl and/or amine terminated) that play an important role not only in the morphology of segmented polyurethane (hard segments of these elastomeric polymers are formed by the reaction between the chain extender and di-isocyanate), but also during

This is an open access article under the terms of the Creative Commons Attribution-NonCommercial-NoDerivs License, which permits use and distribution in any medium, provided the original work is properly cited, the use is non-commercial and no modifications or adaptations are made.

**Correspondence to:** F. Hernández-Sánchez; Unidad de Materiales, Centro de Investigación Científica de Yucatán, A.C., Address: Calle 43 No. 130, Chuburná de Hidalgo, Mérida, Yucatán, México, C.P. 97200; e-mail: fhs@cicy.mx  
Contract grant sponsor: FOMIX; contract grant number: 170132

polyurethane degradation.<sup>7,8</sup> Putrescine is a chemical compound that is present during the natural growth and differentiation of cells.<sup>9,10</sup> Furthermore, its degradation products were shown to have no toxicity to human endothelial cells.<sup>7</sup> Unlike other chain extenders, putrescine is eliminated during the degradation of the PUU copolymer from the body without interfering with its natural processes.<sup>7,11</sup>

The synthesized biodegradable PCL based PUU displayed improved mechanical properties compared with its previously published counterparts; highly tailorable based on the ratio of the incorporated hard (polyurethane) and soft (PCL) segments.<sup>6</sup> By optimizing this ratio, our group has created a PUU copolymer that is capable of approximately 750% deformation before rupture, and possesses an elastic modulus (~70 kPa) ideal for the mechanically demanding environment of cardiac tissue engineering applications.<sup>6</sup>

The aim of this study was to explore whether indirect 3D printing could provide a means to fabricate this novel PCL based PUU polymer into a scaffold suitable for cardiac tissue engineering.

Indirect 3D printing is a novel rapid prototyping technique, where, instead of the final scaffold, a porogen is printed, creating a sacrificial mould, that is then later removed after casting the polymer of interest around it.<sup>12</sup> This method allows types of polymers, such as PUU, to be 3D printed into geometries that may not be achievable using the direct approach.

Techniques based on porogens have been used to obtain scaffolds for tissue engineering before, but these are lacking the ordered architecture that cardiac applications require.<sup>13</sup> In contrast, the indirect printing method it is ideally suited for the controlled creation of the highly organized, aligned micro-architecture and patient specific geometries that cardiac tissue engineering requires that cannot be generated with the traditional methods, such as solvent casting and particle leaching.<sup>12-15</sup>

In this study, 3D printing was used to build porogens from water dissolvable poly(vinyl alcohol) (PVA) with an ordered architecture in three different sizes. This was followed by the pressure-injection of a PUU solution into the porogens. Finally, cylindrical-shaped pieces were cut and immersed in water at room temperature to dissolve the porogen during at least three days.

PUU scaffolds were thus obtained in three different sizes: to contain 300, 400, and 500  $\mu\text{m}$  channels (denoted as PUU-S300; PUU-S400, and PUU-S500, respectively). The generated scaffolds were characterized for their compressive and tensile mechanical behavior; their degradation under simulated physiological conditions was monitored for 12 months; and their architecture, and its correlation to the original porogen structure, was examined using scanning electron microscopy. This was followed by an assessment of the scaffolds performance in cardiac tissue engineering applications, by examining their compatibility with cardiac myocytes and novel cardiac engineering-related techniques, such as aggregate seeding and bi-directional perfusion.

## MATERIALS AND METHODS

### The synthesis of polyurethane-urea

The polymerization of segmented PUU was carried out at 60°C under constant stirring. A solution of PCL-diol (poly-

caprolactone diol,  $M_n \approx 2000$ , Sigma Aldrich, St. Louis, MO) and HMDI (4,4'-Methylenebis(cyclohexyl isocyanate), Sigma Aldrich, St. Louis, MO) in DMF (N,N'-dimethylformamide, Sigma Aldrich, St. Louis, MO) (80% w/v) was placed in a three-neck reactor with Sn-octoate (Sigma Aldrich, St. Louis, MO) (0.2%) for 3 hours. The solution was allowed to cool down to room temperature, after which putrescine (1,4-diaminobutane, Sigma Aldrich, St. Louis, MO) was added drop wise under vigorous stirring, keeping the reaction at room temperature for 1 hour. Finally, the solution was re-heated to 60°C for 1 hour and poured into distilled water, forming a white precipitate. After 30 min, the polymer was removed, washed repeatedly with an ethanol/water mixture (75:25, v/v), and dried under vacuum for 24 h at 60°C. The molar proportion of (PCL-diol: HMDI: putrescine) was (1:2:1).

### Fourier transform infrared (FTIR) spectroscopy and molecular mass

FTIR spectroscopy and gel permeation chromatography (GPC) were performed to verify the correct synthesis of PUU. Infrared spectrum was obtained in a Nicolet Protege 460 FTIR spectrometer. Spectra were collected using a film over a KBr tablet; samples were scanned from 4000 to 500  $\text{cm}^{-1}$ . Polymer molecular mass ( $M_w$ ) was determined in an Agilent Gel Permeation Chromatograph (GPC) model 1100, with DMF (HPLC grade) as the eluent, at 1 mL/min at 50°C. Polystyrene was used as the standard.

**Mechanical testing.** Rectangular samples ( $50 \times 5 \times 0.1$  mm) were cut from films of the synthesized PUU, and placed under tension until rupture in a Shimadzu universal testing machine model AGS-X. The crosshead speed was 100 mm/min, and a load cell of 1000N was employed. Elastic modulus ( $E$ ), ultimate strength ( $\sigma_u$ ), and ultimate deformation ( $\epsilon_u$ ) were calculated.

### The design and fabrication of the porogens

The 3D CAD models of a "woodpile structure" were generated in three different sizes in the OpenSCAD software and converted into the "STL" file format. The woodpile architecture was chosen, as it was hypothesized to lead to a scaffold morphology favorable to cardiac tissue. The three different sizes were created to enable the generation of scaffolds with pore sizes of approximately 300, 400, and 500  $\mu\text{m}$ . Porogens were fabricated based on these three models using a Replicator 3D printer (Makerbot, Brooklyn, NY) and polyvinyl alcohol (PVA) filaments. PVA was selected as the material for the porogens due to its high water solubility, biodegradability and biocompatibility,<sup>16</sup> and as it has been previously used for tissue engineering applications.<sup>17</sup>

### Scaffold fabrication

PUU was dissolved in DMF at 100°C for 3 h under constant stirring. The solution was poured over the porogen in a mould and injected using a nitrogen gas injection system at 4.92  $\text{kgcm}^2$ . The injected polymer was allowed to cool down to room temperature. Scaffolds samples were cut into cylinders ( $\text{Ø}10 \times 5$  mm) and dried under vacuum at 60°C for 24 h. The PVA porogen was completely removed by placing

the scaffold into distilled water, performing two water changes over a 3-day period. Finally, samples were sonicated for 10 minutes to remove any remaining PVA. The samples were dried at room temperature for 1 week, and then dried at 60°C under vacuum for 24 h prior to characterization.

### Scaffold characterization

**Scanning electron microscopy (SEM) and pore size determination.** In order to characterize the morphology of the deposited porogen fibers and the architecture of the PUU scaffolds, samples were coated with gold and visualized under a JEOL JSM-59101LV electron microscope. At least three SEM micrographs were taken at different zones of five of each scaffold type and representative morphologies were reported. Pore size was calculated by at least 20 measures of pores in SEM images, by using the ImageJ analysis software. The area of each pore was measured and then was parameterized to a circular area, to obtain an equivalent diameter, which is called the pore size. Mean and standard deviation values are reported.

**Compression and tensile mechanical testing.** The compression testing of the PUU scaffolds was performed in an Instron 3344 universal testing machine at 1 mm/min until 50% strain using a 100N load cell. Cylindrical-shaped samples (5 mm × 10 mm, H × Ø) were used for each test ( $n = 5$ ). The load was applied along the longitudinal pore direction. Two conditions of PUU scaffolds were tested: dried and wet (48 h in phosphate buffered saline). The compressive secant modulus was calculated at 20% strain ( $E_{20}$ ), as this is the typical level of deformation applied in mechanically stimulated tissue cultures.<sup>18</sup>

Tensile testing was performed in a Shimadzu universal testing machine model AGS-X with a load cell of 100N. This experiment was carried out in order to evaluate the elastic modulus of the samples by applying the load in the XY and the XZ planes. About 30 mm high samples with a 5 mm × 5 mm base were used for XZ plane tests, while 5 mm × 5 mm base × 15 mm high specimens were applied in XY plane measurements. The scaffolds were initially strained to 30% of their original length in order to calculate the secant modulus at 20% deformation, and to measure the residual deformation of the samples in both planes. A strain rate of 2 mm/min was used for samples in the XZ plane, and 1 mm/min was applied in the XY plane. The same samples were used to evaluate the scaffolds' mechanical behavior up to breaking. A crosshead speed of 50 mm/min was used in the XZ plane, and of 20 mm/min in the XY plane. The elastic modulus (20% strain,  $E_{20}$ ), maximum tensile strength ( $\sigma_u$ ), and the elongation at rupture ( $\epsilon_u$ ) were determined.

**Porosity.** The density of the PUU and the porosity of the scaffolds were measured using a Mettler Toledo density kit based on the Archimedes principle of buoyancy.<sup>19</sup>

**Degradation under static simulated physiological conditions.** This experiment was conducted to measure how the molecular weight ( $M_w$ ) of the PUU, and the elastic modulus and mass of the scaffolds change during 12 months under simulated physiological conditions. Samples ( $n = 3$ ) of PUU-S300 were used. Mw measurements were performed on Ø10 × 5 mm cylindrical samples using GPC each month. The mass of the scaffolds was measured at the start, and during each month, of the experiment. Elastic modulus tests (sample size was 10 × 10 mm, Ø × H) were performed every 3 months. Samples were placed in vials with 5 mL of PBS (pH 7.4) with 0.05% of TWEEN® 20 at 37°C. PBS was changed every week.

In order to determine, whether degradation would compromise with time the scaffolds' ability to function in the demanding mechanical environment of the heart, the elastic modulus of the scaffolds was tested using a Perkin Elmer DMA-7 dynamic mechanical analyzer in compression mode. Isothermal tests were conducted at 37°C, with a frequency sweep between 0.5 and 10 Hz. The static load was 200 mN and dynamic load was 50 mN. Elastic modulus was determined at 2 Hz, which is a frequency similar to the normal cardiac rhythm.

### Suitability for cardiac tissue engineering

In order to assess the scaffolds' practical suitability for cardiac tissue engineering, the scaffolds were tested for biocompatibility and in novel cardiac tissue engineering related techniques: cell aggregate seeding and bi-directional perfusion.

**Scaffold pre-treatment.** Prior to cell seeding, PUU scaffolds were sterilized using ethanol, antibiotics, and UV exposure.

**Cardiac myocyte adhesion and viability.** Primary human cardiac myocytes (HCMs) were obtained commercially (Promocell, Germany) and cultured in myocyte growth media (MGM) (Promocell, Germany) at 5% CO<sub>2</sub> and 37°C. Cells were sub-cultured when reaching 80% confluence, and used for experiments at passage 5.

In order to determine whether uncoated PUU can provide a suitable adhesion site alone, or whether pre-coating with extracellular matrix molecules is necessary, cardiac myocytes were cultured on uncoated and fibronectin coated 400 µm PUU scaffolds ( $n = 3$ ), and assayed using the Presto Blue technique after 24 h.

This initial test of cell adhesion, was followed by more thorough examination of whether the scaffolds can maintain the viability of the cells, and whether channel size might have an influence on this. 300, 400, and 500 µm scaffolds were incubated with fibronectin (50 µg/mL, Sigma Aldrich, UK) and seeded with 100 µL of MGM containing  $1 \times 10^5$  cells ( $n = 3$ ). For the controls, the same amount of cells was seeded directly into the wells of a standard culture plate. After 1 hour of incubation, 1 mL of MGM was added to each sample, which were then cultured at 37°C and 5% CO<sub>2</sub> for 90 min and 24 hours. The Presto Blue cell viability and the

PicoGreen cell number assays were used for the evaluation of the samples.

**Cell aggregate seeding.** Cell aggregates were obtained by trypsinization and incubation of HCMs in GravityPLUS plates (Insphero, Switzerland). Fibronectin coated scaffolds were seeded either by cell suspension (CS) or by cell aggregates (CA) at  $4 \times 10^4$  cells per scaffold (equivalent to  $2 \times$  cell aggregates per scaffold), as this is the recommended cell number that allows viable cell aggregates to form that are optimal for seeding. The seeded scaffolds were cultured up to seven days, with time points at day 3 and day 7 for CellTracker imaging, cardiac  $\alpha$ -actin staining, and the PicoGreen assay ( $n = 3$ ).

**Bi-directional perfusion seeding.** PUU scaffolds were sterilized and coated with fibronectin, after which they were placed in a TEB-1000 perfusion bioreactor (Ebers, Spain). The scaffolds were seeded with 10,000 cells per scaffold in duplex mode at 0.1 mL/s flow rate. Static seeded scaffolds were used as the control. Post-seeding, the scaffolds were incubated for 2 hours, and assayed using the Presto Blue kit and SEM ( $n = 2$ ) in order to examine the efficiency of the seeding.

#### Biological assays

**Cell viability: Presto blue assay.** Scaffolds were placed into a fresh 24-well plate, washed with PBS and incubated in a 10% solution of Presto Blue at 37°C for 30 min. The solution was transferred into a 96-well plate in replicates, and absorbance was measured in a plate reader at 570 nm excitation and 600 nm emission.

**Cell numbers: PicoGreen assay.** Cell numbers in the seeded scaffolds were measured using the Quant-iT PicoGreen dsDNA Assay kit (Life Technologies, The United States). The scaffolds were placed in Eppendorf tubes and 1 mL of  $1 \times$  TE buffer (included in kit) was added per sample. The samples were frozen at  $-80^\circ\text{C}$ , followed by two cycles of freeze-thaw in order to ensure the complete lysis of the cells. About 100  $\mu\text{L}$  of the lysate was added to wells of 96-well plates and mixed with 100  $\mu\text{L}$  of the stain solution (prepared according to the manufacturer's instruction). Fluorescence was read at 485 nm excitation and 528 nm emission.

**CellTracker imaging.** In order to track the cells' adhesion to the scaffolds, HCMs were dyed with CellTracker Green (Life Technologies, The United States), a non-toxic stable fluorescent probe that is transferred to daughter cells, and were imaged using a confocal microscope (Leica TCS SPE, Germany).

**Cardiac  $\alpha$ -actin staining.** Cellular phenotype was confirmed through cardiac  $\alpha$ -actin staining, a marker for contractile heart muscle cells,<sup>20</sup> using mouse anti-cardiac- $\alpha$ -actin (Sigma-Aldrich, The United Kingdom) and a goat anti-mouse Alexa fluor 555 secondary antibody. Nuclear staining

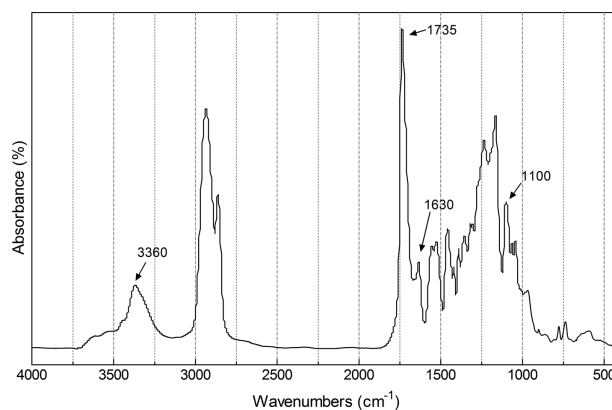


FIGURE 1. FTIR spectrum of the synthesized PUU polymer.

was performed using Vectashield-DAPI (Vector Laboratories, #H-1500).

#### Statistical analysis

Results are represented as mean  $\pm$  standard deviation, and were analyzed using One-way ANOVA with Tukey's post-test and Two-way ANOVA followed by Bonferroni's post-test (Minitab v16.1, GraphPad Prism v5). A "p" value equal to, or smaller than, 0.05 was considered significant.

## RESULTS

### Polyurethane-urea

FTIR spectroscopy of the synthesized polymer confirmed that it is PUU (Fig. 1), with the pronounced carbonyl peak of the ester in the urethane groups and in the soft segment at  $1735\text{ cm}^{-1}$ , and a shoulder peak at  $1630\text{ cm}^{-1}$  attributable to the urea carbonyl groups. The urethane and urea groups also showed absorbance at  $3360\text{ cm}^{-1}$ . The absorbance at  $1100\text{ cm}^{-1}$  was attributed to the ether in the soft segment. The absence of a peak at  $2267\text{ cm}^{-1}$  indicated the lack of unreacted isocyanate groups.

The mechanical properties and molecular mass of the PUU are shown in Table I. The synthesized polymer proved to be highly deformable and to have a low elastic modulus, giving it good mechanical properties for soft tissue engineering applications.

### Scaffold characterization

**Scanning electron microscopy.** Examination of the porogens under SEM has shown that the frameworks printed out of 300 and 400  $\mu\text{m}$  fibers (Fig. 2) were completely aligned. However, those printed to provide 500  $\mu\text{m}$  channels displayed a distorted morphology: The newly deposited

TABLE I. Tensile and Physicochemical Properties of the Synthesized Segmented PUU

Elastic modulus ( $E$ )	$5.76 \pm 2.85$	MPa
Ultimate strength ( $\sigma_u$ )	$30.13 \pm 7.43$	MPa
Ultimate deformation ( $\epsilon_u$ )	$692.46 \pm 78.76$	%
Contact angle	$92.5 \pm 2.9$	$^\circ$
Molecular weight	$7.2455 \times 10^5$	g/mol

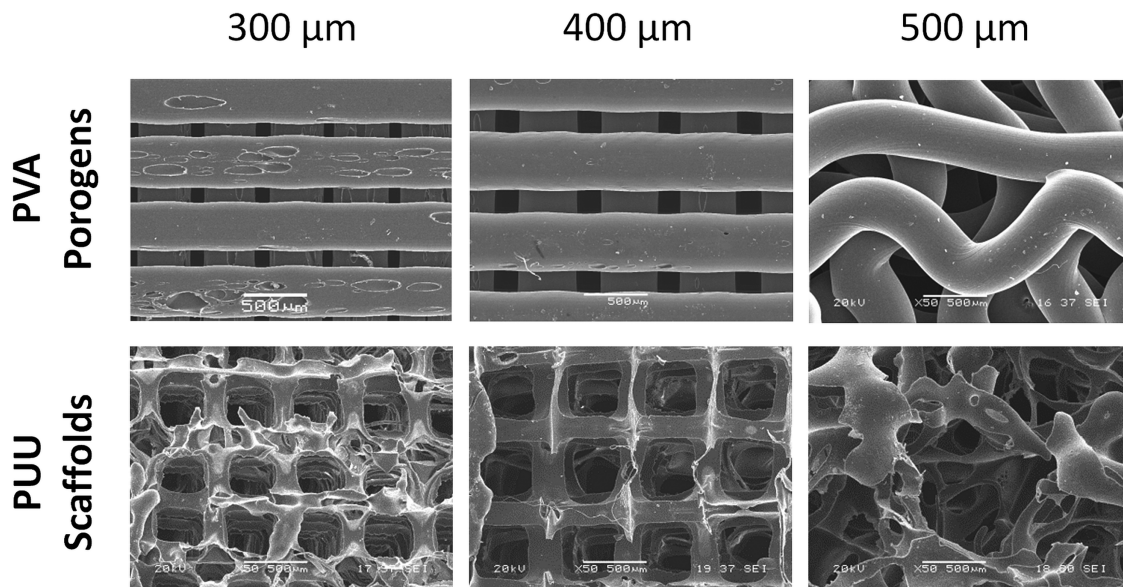


**FIGURE 2.** SEM images of the PVA porogens in the three different sizes (above) and the PUU scaffolds (below) that they generated. The displayed images were taken of the XY plane of the porogens/scaffolds (parallel to the fiber/channel direction). The stacks of 300 and 400  $\mu\text{m}$  thick porogens created aligned channels in the PUU scaffolds. The 500  $\mu\text{m}$  thick porogens deformed under their own weight, resulting in a distorted scaffold architecture. The scale bar represents 500  $\mu\text{m}$ .

porogen fibers bent around the already consolidated ones, creating a wavy fiber morphology.

SEM images of the scaffolds (Fig. 2) show a network of aligned channels in the XZ and YZ planes, connected by rectangular pores in the XY plane, in case of the 300 and 400  $\mu\text{m}$  pore PUU scaffolds.

The 500  $\mu\text{m}$  scaffolds contained semi-aligned channels in the XZ and YZ planes that, unlike with the other two scaffold types, do not provide an unobstructed straight path through the scaffold. In the XY plane, instead of the rectangular pores observed with the 300 and 400  $\mu\text{m}$  scaffolds, a random architecture was detected without any visible orientation or alignment.

The inner walls of the channels displayed a rough, irregular morphology with micro-pores along the surface in the case of all three scaffold types.

**Mechanical properties.** Figure 3 shows the mechanical behavior of the three different scaffold types under both dry and wetted conditions during compression testing. The recorded curves display the three typical stages of the compression of porous materials. Elastic bending of the pore walls in the scaffolds is present in the first stage (from 0% to 20% of strain); followed by a plateau dominated by elastic buckling of the pore walls; finally, an increase in stiffness is shown as a result of the collapse of the foam structure.<sup>21</sup>

The compressive modulus of the 300 and 400  $\mu\text{m}$  channel scaffolds was found not to be statistically different. However, the value was observed to drop from approximately 11 to 4–7 kPa once the scaffolds were wetted. The 500  $\mu\text{m}$  scaffolds displayed a significantly higher compressive modulus compared with its two counterparts, with a

value of approximately 15.6 kPa when dry, and 13.3 kPa when wetted.

The scaffolds displayed anisotropic behavior under tension, with higher stiffness (an elastic modulus of  $\sim 132$  kPa) in the XZ plane (perpendicular to the direction of the channels), and higher elasticity (elastic modulus of  $\sim 15$  kPa) in the XY plane (parallel to the channels). The ultimate deformation that the scaffolds reached was not statistically different between the two planes. The residual strain of the scaffolds subjected to a 39% strain was less than 3%.

**Porosity.** Porosity measurements (Table II) have shown that not only the diameter of the channels, but also the variability of the pores sizes, increased with the thickness of the porogens. The greatest variability in pore size was detected in the case of the 500  $\mu\text{m}$  scaffolds. This was probably due to the deformation and misalignment of the fibers as detected by SEM.

**Degradation.** The molecular mass of polymer was reduced by one order of magnitude (from  $10^5$  to  $10^4$  g/mol) during the 12-month period (see Fig. 4), whereas the mass loss remained practically unchanged (lower than 5%). This fact could be attributed to an induction phase of degradation, in which the polymers undergo random scission of chains without significant loss of physical mass. The degradation kinetics of segmented polyurethane depends on the polymer's chemical structure. In other words, depends upon the reagents used during synthesis of the PUU, that is, the type of chain extender, the type of isocyanate or polyol, and/or the synthesis conditions. The findings of this study regarding the degradation kinetics of PUU are similar to those presented in the scientific literature.<sup>22,23</sup>

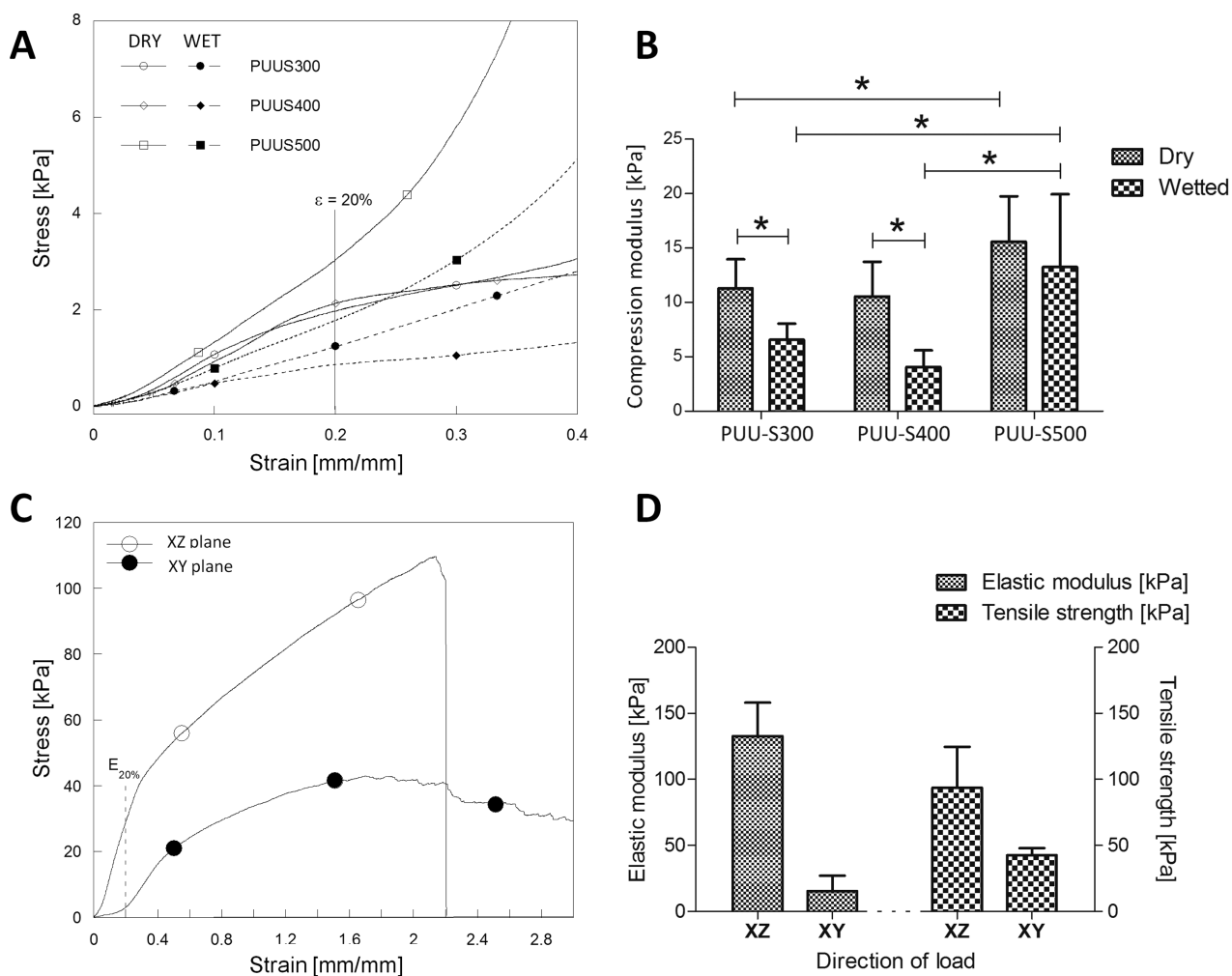


**FIGURE 3.** The compression and tensile mechanical properties of the PUU scaffolds: The compression stress-strain curves (A) and moduli (B) of all three scaffold types under both dry and wet conditions. The tensile stress-strain curve (C), elastic modulus and tensile strength (D) of a 400  $\mu\text{m}$  scaffold in both the XY (parallel to channels) and XZ (perpendicular to channels) planes. Statistically significant differences ( $p < 0.05$ ) are denoted by the “\*” symbol.

The dynamic mechanical evaluation of the samples demonstrated an increase in the storage modulus ( $E'$ ) of the scaffolds from 1.5 to 2.8 MPa by the end of month 12.

### Suitability for cardiac tissue engineering

**Cardiac myocyte adhesion and viability.** After 24 hours of static culture fibronectin coated scaffolds showed 94% viability (Fig. 5), while uncoated scaffolds produced a significantly reduced value of 65%, compared with two-dimensional (2D) tissue culture plastic controls. Therefore, in all following experiments the scaffolds were pre-coated with fibronectin before use.

When comparing the cellular adhesion to the three different scaffold types and to 2D tissue culture plastic controls, no significant difference was found between the scaffolds and the control samples after 90 min and 24 h (Fig. 6).

**Cell aggregate seeding.** CellTracker fluorescent staining revealed that the cells have spread out across the scaffolds in a near homogenous manner with both suspension and aggregate seeding strategies.

Cell aggregate seeded scaffolds showed significantly higher cell numbers ( $p < 0.001$ ) at day 3 and 7 compared

**TABLE II. The Porosity of all Tree Scaffold Types**

Parameter	Unit	PUU-S300	PUU-S400	PUU-S500
Average pore diameter (XZ plane)	$\mu\text{m}$	$338.54 \pm 140.78$	$433.03 \pm 144.75$	$478.26 \pm 251.79$
Average pore diameter (XY plane)	$\mu\text{m}$	$363.22 \pm 30.44$	$517.98 \pm 57.90$	$599.93 \pm 319.93$
Overall porosity	(%)	$96.33 \pm 0.69$	$92.57 \pm 0.66$	$92.04 \pm 1.13$

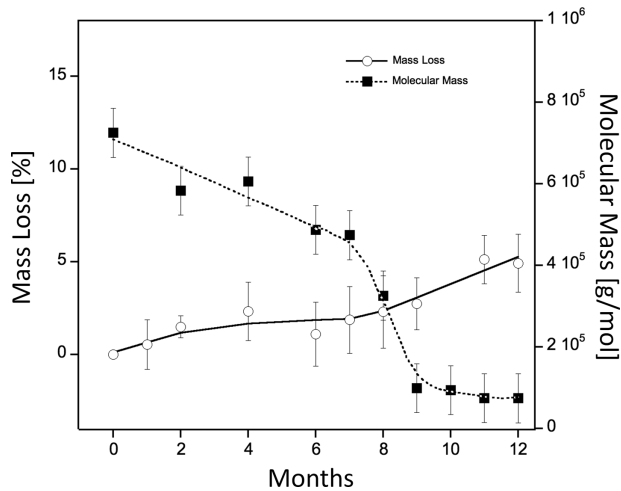


**FIGURE 4.** The degradation of PUU scaffolds under simulated physiological conditions monitored in terms of mass loss (left axis, *clear circles*) and molecular weight (right axis, *full squares*) up to 12 months.

with cell suspension seeded samples and two dimensional tissue culture plastic (TCP) control cultures (Fig. 7). Furthermore, the cells in these scaffolds appeared to grow into the channels, leaving the walls of the scaffold. The cells seeded in suspension, although less proliferative than the aggregate cultures, performed equivalently to TCP controls. Furthermore, suspension seeded cells appeared to form longer and more mature myofibers than the aggregates, indicating the possibility of generating a more functional tissue construct. Immunostaining of the scaffolds for cardiac  $\alpha$ -actin showed that the cells have maintained their phenotype with both seeding methods during the seven days of the culture (Fig. 8).

**Bi-directional perfusion seeding.** Bi-directional perfusion markedly increased the seeding efficiency in the case of all three scaffold types compared with static controls (Fig. 9). The difference between static and perfused samples was largest in the case of the 500  $\mu$ m scaffolds, showing a 1.5

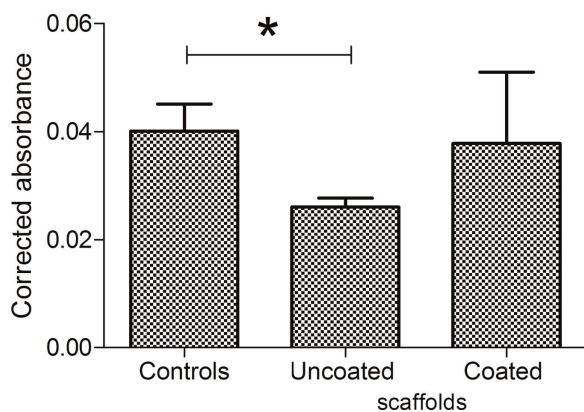


**FIGURE 5.** The viability of cardiac myocytes after 24 h on fibronectin coated and uncoated PUU scaffolds, and 2D tissue culture plastic controls was tested using the PrestoBlue assay ( $n = 3$ ). Statistically significant differences ( $p < 0.05$ ) are denoted by the “\*” symbol.

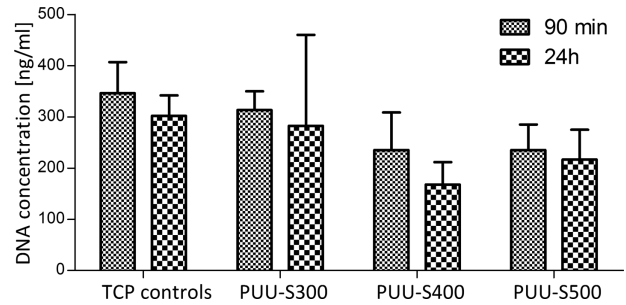


**FIGURE 6.** DNA content of all three PUU scaffold types and tissue culture plastic (TCP) controls after both 90 min and 24 h ( $n = 3$ ).

times greater average efficiency in favor of perfusion. SEM has demonstrated that, in contrast with static cultures, where cells remained more toward the surface, cells penetrated deeper into the scaffolds with perfusion, adhering to the walls of the channels.

## DISCUSSION

The aim of this study was to explore whether indirect 3D printing can be used as a method for fabricating a novel PUU variant into scaffolds suitable for cardiac tissue engineering.

A wood stack structure was chosen as the basis of the progenes, as it would yield an anisotropic structure of aligned channels. Such architecture was hypothesized to provide excellent support for the formation of cardiac myofibrils; promote homogenous tissue growth through excellent nutrient/waste exchange; and to provide a means to mimic the anisotropic mechanical properties of heart muscle.

SEM of the scaffolds has demonstrated that this architecture was successfully created through indirect printing. The size of the channels in the PUU structures correlated well with the thickness of the printed PVA filaments on average, however there was a relatively large standard deviation (in the range of  $\pm 140$ – $200 \mu$ m) present. This was largest with the 500  $\mu$ m scaffolds, which is understandable considering that, as the SEM images have shown, the PVA filaments at this thickness were unable to support their weight and collapsed, generating a distorted scaffold morphology. The

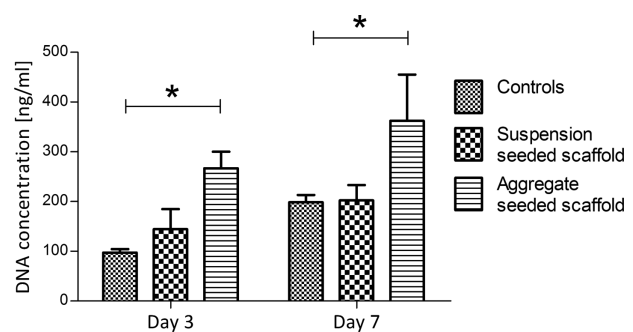


**FIGURE 7.** DNA concentration in cell suspension and cell aggregate seeded PUU scaffolds and in TCP control samples after three and seven days of culture ( $n = 3$ ). The scaffolds and controls were seeded under static conditions. Statistically significant differences ( $p < 0.05$ ) are indicated by the “\*” symbol.

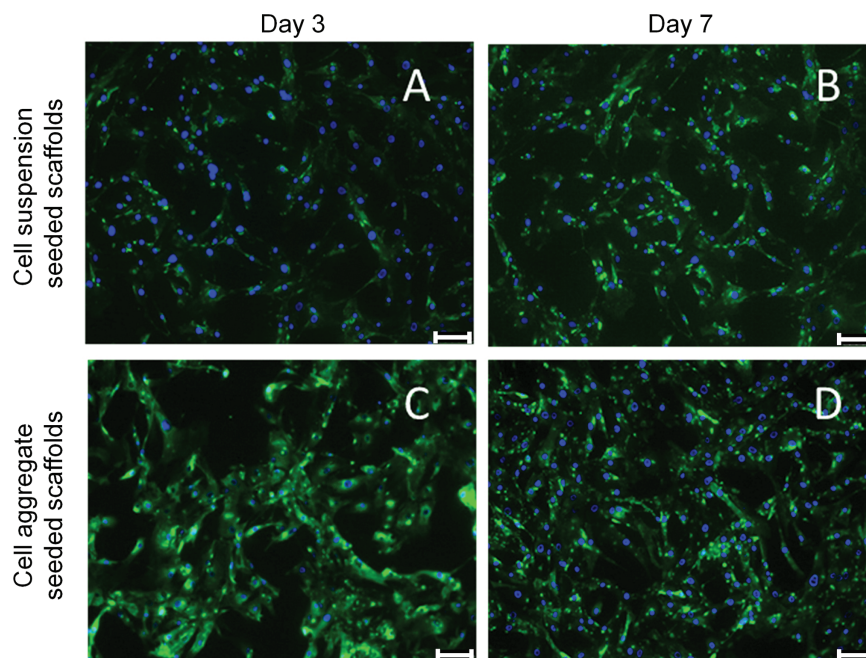


**FIGURE 8.** Confocal microscopy images of cardiac  $\alpha$ -actin (a marker of cardiac myocytes) and DAPI (cell nucleus) stained sections of cell suspension and cell aggregate seeded PUU scaffolds after 3 and 7 days in culture. The scale bar represents 25  $\mu$ m.

distortion highlights the fact that there are some limitations to this rapid prototyping technique, and that the mechanical properties of the porogen material has to be kept in mind when choosing the geometry of the scaffold.

A requirement for any cardiac scaffold that it should offer no resistance to the muscle's contraction during the systole, while providing mechanical support to the tissue against the tensile stresses of the diastolic phase.<sup>24</sup> The created scaffolds fulfill both of these criteria: The elastic modulus of 15–132 kPa displayed by the scaffolds under tension fits well into the range measured for cardiac muscle 20–500 kPa,<sup>24</sup> and resides within the interval (7.9–1200 kPa) that

has been reported in previous cardiac biomaterial studies.<sup>25–30</sup>

Furthermore, thanks to the low compression modulus shown by the wetted scaffolds (4–13.5 kPa), it is expected that the constructs will offer very little resistance to the contraction of the cardiomyocytes. Additionally, it is also expected that the scaffolds will not lose their geometry once in use, as they are capable of almost completely regaining their original shape even after high levels of deformation, demonstrated by the very low residual strain (3%) remaining in the samples after stretching them by 39%.

The scaffolds degraded slowly, losing only 5% of their mass by the end of a 12-months period. However, these values are not unlike that of the currently commercially available counterparts. For example, the polyurethane based thumb joint implant, Artelon Artimplant, requires 6 years to break down *in vivo*.<sup>6</sup> Furthermore, considering that the molecular weight of the PUU has dropped to almost one tenth of its original value by the end of the 12 months, it is highly likely that the scaffolds will erode much faster once exposed to the constant compression-tension cycles present in the mechanically demanding environment of the heart muscle.

The PUU scaffolds displayed good biocompatibility, maintaining cardiac myocyte viability equivalently to tissue culture plastic once coated with fibronectin. Cell numbers were reduced in all scaffold types after 24 h compared with tissue culture plastic controls, however this was found not to be statistically significant, and is not unlike the findings of similar PU studies.<sup>31</sup> On the other hand, in cell aggregate seeding experiments the scaffold samples showed higher proliferation compared with TCP controls at both time

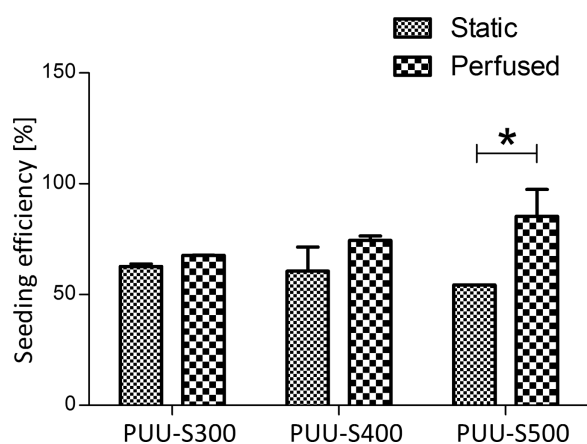


**FIGURE 9.** The efficiency of bi-directional perfusion compared with static seeding in the case of all three scaffold types measured using the PrestoBlue assay ( $n=2$ ). Statistically significant differences ( $p < 0.05$ ) are indicated by the “\*” symbol.



points, containing three times as much cells after 3 days and twice as much after 7 days. This not only demonstrates that the cells are capable of recovering after an initial period of low proliferation, but also emphasizes the benefits of cell aggregate seeding and the excellent compatibility of the PUU scaffolds with this novel technique. Fluorescent imaging showed that the cells have spread out evenly across the scaffold. This is significant considering that with most scaffolds, cells tend to distribute in a heterogeneous manner, favoring the surface of the constructs.<sup>32,33</sup>

Furthermore, the cells maintained their contractile myocardial phenotype up until 7 days, as demonstrated by cardiac  $\alpha$ -actin staining, showing that PUU is capable of maintaining not only viability, but also differentiation. The scaffolds performed well in perfusion experiments, displaying no limitation in this regard. Interestingly, perfusion seeding made the greatest difference in the case of the 500  $\mu$ m scaffolds. This is understandable, however, as the distorted geometry of this scaffold type, although makes cell penetration more difficult under static condition, is beneficial for capturing cells once perfused. However, the intricate internal morphology of the distorted 500  $\mu$ m scaffolds is not beneficial considering the requirements of cardiac tissue engineering post-seeding, where it may disrupt uniform medium flow through the scaffold and block the formation of myofiber strands. In contrast, the uniform channels and even porosity of the PUU-S300 and 400 scaffolds are ideally suited for this,<sup>34</sup> making them promising candidates as cardiac scaffolds.

## CONCLUSIONS

In summary, our findings demonstrate the potential of combining indirect rapid prototyping and elastomeric segmented polyurethane-urea as a means to fabricate soft scaffolds with controlled 3D micro-architecture and pore size for cardiac tissue engineering.

The produced scaffolds were found to have excellent mechanical properties, being strong enough to withstand the tensile stresses of the diastole, while offering very little resistance to the contraction of the tissue during systole. The material showed good biocompatibility with cardiac myocytes, outperforming tissue culture plastic in term of cell numbers after only three days in culture. Furthermore, the cells incorporated into the scaffolds preserved their contractile myocardial phenotype with no signs of de-differentiation. The constructs worked well in perfusion experiments, showing enhanced seeding efficiency.

Further *in vitro* investigations will follow, combining aggregate seeding, perfusion, and mechanical stimulation in longer-term experiments, and testing additional geometries, in order to provide further evidence of the potential that this biomaterial and novel scaffold fabrication technique has for cardiac tissue engineering.

## ACKNOWLEDGMENT

To Consejo Nacional de Ciencia y Tecnología (CONACYT), México, by scholarship to Roberto Hernández-Córdova, and to Consejo de Ciencia, Innovación y Tecnología del Estado de

Yucatán (CONCITEY) by financial support for Research Project Grants, FOMIX-170132. The authors would like to thank Mr Glen Ferris for his technical support.

## REFERENCES

1. Chiu LLY, Radisic M. Cardiac tissue engineering. *Curr Opin Chem Eng* 2013;2:41–52.
2. Barton P, Andronis L, Briggs A, McPherson K, Capewell S. Effectiveness and cost effectiveness of cardiovascular disease prevention in whole populations: Modelling study. *BMJ* 2011;343:d4044.
3. Taylor DA, Sampaio LC, Gobin A. Building new hearts: A review of trends in cardiac tissue engineering. *Am J Transplant* 2014;14:2448–2459.
4. Boffito M, Sartori S, Ciardelli G. Polymeric scaffolds for cardiac tissue engineering: Requirements and fabrication technologies. *Polym Int* 2014;63:2–11.
5. Generali M, Dijkman PE, Hoerstrup SP. Bioresorbable scaffolds for cardiovascular tissue engineering. *EMJ Int Cardiol* 2014;1:91–99.
6. May-Hernández L, Hernández-Sánchez F, Gómez-Ribelles JL, Sabater Serra R. Segmented poly(urethane-urea) elastomers based on polycaprolactone: Structure and properties. *J Appl Polym Sci* 2011;119:2093–2104.
7. Guan J, Sacks MS, Beckman EJ, Wagner WR. Synthesis, characterization, and cytocompatibility of elastomeric, biodegradable poly(ester-urethane)ureas based on poly(caprolactone) and putrescine. *J Biomed Mater Res* 2002;61:493–503.
8. Hong Y, Guan J, Fujimoto KL, Hashizume R, Pelinescu AL, Wagner WR. Tailoring the degradation kinetics of poly(ester-carbonate urethane)urea thermoplastic elastomers for tissue engineering scaffolds. *Biomaterials* 2010;31:4249–4258.
9. Tabor CW, Tabor H. 1,4-diaminobutane (putrescine), spermidine and spermine. *Annu Rev Biochem* 1976;45:285–306.
10. Cauch-Rodríguez JV, Chan-Chan LH, Hernández-Sánchez F, Cervantes-Uc JM. Degradation of polyurethanes for cardiovascular applications. In: Pignatello R, editor. *Advances in Biomaterials Science and Biomedical Applications*. Croatia: InTech; 2013. p 51–82.
11. Guan J, Sacks MS, Beckman EJ, Wagner WR. Biodegradable poly(ether ester urethane)urea elastomers based on poly(ether ester) triblock copolymers and putrescine: Synthesis, characterization and cytocompatibility. *Biomaterials* 2004;25:85–96.
12. Park JH, Jung JW, Kang HW, Cho DW. Indirect three-dimensional printing of synthetic polymer scaffold based on thermal molding process. *Biofabrication* 2014;6:1–10.
13. Lebourg M, Sabater Serra R, Más Estellés J, Hernández-Sánchez F, Gómez-Ribelles JL, Suay Antón J. Biodegradable polycaprolactone scaffold with controlled porosity obtained by modified particle-leaching technique. *J Mater Sci: Mater Med* 2008;19:2047–2053.
14. Yeong W-Y, Chua C-K, Leong K-F, Chandrasekaran M. Rapid prototyping in tissue engineering: Challenges and potential. *Trends Biotechnol* 2004;22:643–652.
15. Yeong WY, Sudarmadji N, Yu HY, Chua CK, Leong KF, Venkatraman SS, Boey YC, Tan LP. Porous polycaprolactone scaffold for cardiac tissue engineering fabricated by selective laser sintering. *Acta Biomater* 2010;6:2028–2034.
16. Ghanbarzadeh B, Almasi H. Biodegradable polymers. In: Chamy R, Rosenkranz F, editors. *Biodegradation – Life of Science*. Rijeka: InTech; 2013. p 141–185.
17. Vrana NE, Liu Y, McGuinness GB, Cahill PA. Characterization of poly(vinyl alcohol)/chitosan hydrogels as vascular tissue engineering scaffolds. *Macromol Symp* 2008;269:106–110.
18. Akhyari P, Fedak PWM, Weisel RD, Lee T-YJ, Verma S, Mickle DAG, Li R-K. Mechanical stretch regimen enhances the formation of bioengineered autologous cardiac muscle grafts. *Circulation* 2002;106:1-137–1-142.
19. Pickover C. *Archimedes to Hawking: Laws of Science and the Great Minds Behind Them*. Oxford: Oxford University Press; 2008. 528 p.
20. Müller M, Mazur AJ, Behrmann E, Diensthuber RP, Radke MB, Qu Z, Littwitz C, Raunser S, Schoenenberger C-A, Manstein DJ, Mannherz HG. Functional characterization of the human  $\alpha$ -cardiac actin mutations Y166C and M305L involved in hypertrophic cardiomyopathy. *Cell Mol Life Sci* 2012;69:3457–3479.

21. Gibson LJ, Ashby MF, Harley BA. *Cellular Material in Nature and Medicine*. Cambridge: Cambridge University Press; 2010. 309 p.
22. Chan-Chan LH, Solis-Correa R, Vargas-Coronado RF, Cervantes-Uc JM, Cauich-Rodríguez JV, Quintana P, Bartolo-Pérez P. Degradation studies on segmented polyurethanes prepared with HMDI, PCL and different chain extenders. *Acta Biomater* 2010;6:2035–2044.
23. Chan-Chan LH, Tkaczyk C, Vargas-Coronado RF, Cervantes-Uc JM, Tabrizian M, Cauich-Rodríguez JV. Characterization and biocompatibility studies of new degradable poly(urea)urethanes prepared with arginine, glycine or aspartic acid as chain extenders. *J Mater Sci: Mater Med* 2013;24:1733–1744.
24. Chen Q-Z, Bismarck A, Hansen U, Junaid S, Tran MQ, Harding SE, Ali NN, Boccaccini AR. Characterisation of a soft elastomer poly(glycerol sebacate) designed to match the mechanical properties of myocardial tissue. *Biomaterials* 2008;29:47–57.
25. Courtney T, Sacks MS, Stankus J, Guan J, Wagner WR. Design and analysis of tissue engineering scaffolds that mimic soft tissue mechanical anisotropy. *Biomaterials* 2006;27:3631–3638.
26. Chimenti I, Rizzitelli G, Gaetani R, Angelini F, Ionta V, Forte E, Frati G, Schussler O, Barbetta A, Messina E, Dentini M, Giacomello A. Human cardiosphere-seeded gelatin and collagen scaffolds as cardiogenic engineered bioconstructs. *Biomaterials* 2011;32:9271–9281.
27. Araña M, Peña E, Abizanda G, Cilla M, Ochoa I, Gavira JJ, Espinosa G, Doblaré M, Pelacho B, Prosper F. Preparation and characterization of collagen-based ADSC-carrier sheets for cardiovascular application. *Acta Biomater* 2013;9:6075–6083.
28. Chan V, Raman R, Cvetkovic C, Bashir R. Enabling microscale and nanoscale approaches for bioengineered cardiac tissue. *ACS Nano* 2013;7:1830–1837.
29. Fleischer S, Feiner R, Shapira A, Ji J, Sui X, Wagner HD, Dvir T. Spring-like fibers for cardiac tissue engineering. *Biomaterials* 2013;34:8599–8606.
30. Godier-Furnémont AFG, Martens TP, Koeckert MS, Wan L, Parks J, Arai K, Zhang G, Hudson B, Homma S, Vunjak-Novakovic G. Composite scaffold provides a cell delivery platform for cardiovascular repair. *Proc Natl Acad Sci U S A* 2011;108:7974–7979.
31. Chiono V, Mozetic P, Boffito M, Sartori S, Gioffredi E, Silvestri A, Rainer A, Giannitelli SM, Trombetta M, Nurzynska D, Di Meglio F, Castaldo C, Miraglia R, Montagni S, Ciardelli G. Polyurethane-based scaffolds for myocardial tissue engineering. *Interface Focus* 2014;4:20130045.
32. Volkmer E, Drosse I, Otto S, Stangelmayer A, Stengele M, Kallukalam BC, Mutschler W, Schieker M. Hypoxia in static and dynamic 3D culture systems for tissue engineering of bone. *Tissue Eng Part A* 2008;14:1331–1340.
33. Volkmer E, Otto S, Polzer H, Saller M, Trappendrehre D, Zagar D, Hamisch S, Ziegler G, Wilhelmi A, Mutschler W, Schieker M. Overcoming hypoxia in 3D culture systems for tissue engineering of bone in vitro using an automated, oxygen-triggered feedback loop. *J Mater Sci Mater Med* 2012;23:2793–2801.
34. Melchels FPW, Tonnarelli B, Olivares AL, Martin I, Lacroix D, Feijen J, Wendt DJ, Grijpma DW. The influence of the scaffold design on the distribution of adhering cells after perfusion cell seeding. *Biomaterials* 2011;32:2878–2884.